Eur J Med Res (2006) 11: 527-533

Differentiation between Malignant and Benign Solitary Pulmonary Nodules with Proton Density Weighted and ECG-gated Magnetic Resonance Imaging

J. F. Schaefer[1], J. Vollmar[1], J. Wiskirchen[1], B. Erdtmann[1], D. v. Renteln[1], R. Vonthein[2], F. Schick[3], C. D. Claussen[1], M. D. Seemann[1,4]

[1]Department of Diagnostic Radiology Eberhard-Karls-University Tuebingen,
[2]Department of Medical Biometry Eberhard-Karls-University Tuebingen,
[3]Department of Diagnostic Radiology, Section of Experimental Radiology Eberhard-Karls-University Tuebingen,
[4]Department of Radiology and Nuclear Medicine, University of Magdeburg, Germany

Abstract
Objective: To estimate performance of MRI for differentiating malignant from benign solitary pulmonary nodules (SPN) using morphological characteristics.
Material and Methods: MRI in 46 patients with SPN (mean diameter: 19mm) was carried out on 1.0 Tesla scanner using ECG-gated, gradient echo sequence. Morphological signs of SPN were determined and compared with previously performed helical-CT, where final diagnosis served as reference with 52% frequency of malignancy. Furthermore, three observers evaluated all images.
Results: Significant differences between the two groups were found for nodules shape, margin, inhomogeneity and the vessel-sign in MRI, nodules shape, margin, the vessel-sign, and presence of spicules in CT. Using these signs, AUC were 0.746 for MRI and 0.765 for CT. The mean sensitivity, specificity, and accuracy of observers for MRI/CT were 89%/95%, 42%/41%, 66%/68%, respectively.
Conclusions: Despite discrepancies in morphologic appearance, no significant difference of accuracy between MRI and CT was determined. Further investigations are necessary to demonstrate the clinical use in combination with functional parameters, establishing MRI as a comprehensive diagnostic modality for SPN.

Key words: Lung disease; Lung neoplasm; Lung nodule; Magnetic resonance (MR); Computed tomography (CT)

Introduction

Although being a radiation free modality, MRI is not the first choice imaging tool for detection as well as classification of solitary pulmonary nodules (SPN). Two methodical drawbacks predominate: Unfavourable artefacts through pulsation and breathing, and the extremely short T2* relaxation time of normal lung parenchyma (i.e. approximately 1 ms at 1.5 Tesla [1]). Furthermore, the low proton density of lung tissue and the signal dephasing due to pulmonary blood flow hamper imaging [2, 3]. Long examination times, high costs and limited availability have also to be considered.

On the other hand, new developments of MRI technique with the possibility of whole body imaging for screening and for staging malignant tumours, as well as the fusion of morphological and functional imaging, (i.e. PET/MRI as a new modality in the future) motivate research in this field [4-6]. In the past, most of MRI studies have investigated either the detection rate of pulmonary nodules in comparison with CT [7-10] or the characterisation of SPN using dynamic contrast enhanced imaging. The latter approach seems to be a promising technique which reveals a higher accuracy than dynamic contrast CT in differentiating malignant from benign lesions [11-13]. However, the combined evaluation of morphology and enhancement is crucial for efficacy in diagnostic imaging, which has also been shown for SPN in the combined evaluation of CT morphology and MRI enhancement.[14].

The use of ECG-gated and breath-hold MR imaging seems to be a promising technique for pulmonary disorders [3, 10]. The aims of this retrospective study were to evaluate the classical morphological characteristics of malignant and benign SPN using an ECG-gated GE sequence, as well as to compare the diagnostic accuracy with CT, when the reference standard is the final diagnosis.

Materials and Methods

Patients were selected for the presented study from two departments of thoracic surgery if they met the following criteria: (a) presence of a newly detected SPN in CT which needed further evaluation, (b) absence of calcification and definite fat, (c) nodule size of 5 to 40 mm, (d) absence of recent history of pneumonia or immune-deficiency, (e) absence of contraindications for MRI (i.e. pacemaker), and (f) probable ability to cooperate with the procedure.

Forty six patients (10 female, 36 male, age range 26 to 77 years, mean age 61 years) with a SPN ranging in size from 6 to 39 mm (mean 19 $\pm$ 8 mm) were included in the analysis after giving informed consent and following study approval from the Institutional Committee in Medical Ethics. In 43 cases, a histological diagnosis was reached by resection or biopsy whereas in

three patients, a follow-up by CT over a time period of 2 years was completed.

MR Imaging

MR imaging was performed with a 1.0 Tesla MR-Scanner (Magnetom Expert, Siemens, Erlangen, Germany) using the phased array coil as receiver. The thorax was examined from the apex to the base using a transverse, breath hold, ECG gated, proton-density weighted 2D gradient echo sequence (repetition time = 10 ms, echo time = 6 ms, flip = 20°, bandwidth 400 Hz per pixel, voxel size 1.3 mm - 1.3 mm - 6 mm). The GE sequence applied segmented k-space sampling allowing to record raw data for 5 slices in one breath-hold. Recording of raw data for each single image in a set was performed in a specific cardiac phase. This ECG-gated acquisition technique provided lacking flow or cardiac motion related artifacts, even in regions close to the myocardial walls. Care was taken to avoid gaps between the image sets due to variable breathing levels, and overlapping of the slabs was used. Although expiratory breath holds are considered more reproducible, images were recorded in inspiration due to the better delineation of the nodules against inflated lung parenchyma. Patients were requested to hold the same respiratory level for all breath holds. Five to seven breath holds were necessary to cover the entire lung. If the acquisition time was too long due to cardiac rate, the number of slices per slab was reduced. The total examination time for this procedure was approximately 7 to 10 minutes.

CT Imaging

The CT examination was carried out in two clinics and 5 departments of radiology using single row helical CT except in one case, where an incremental CT scan was carried out. Tube current ranged from 110 to 250 mAs with tube voltage of 120 to 140 KV. The referring departments set slice thickness from 5 to 8 mm. Slice increments between 12% and 20% were used. In 31 cases, contrast media (CM) was administered. A standard field of view (approximately 350 mm) was carried out without focusing on lesion site. The CT examination was digitally available in 26 cases. Laser films (14 x 17 inch, layout 4 x 5 images) in both lung and mediastinal window were used in the remaining cases.

Image Evaluation of SPN

The image analysis of MRI and CT was carried out on a commercial viewing platform (Siemens Syngo, Siemens, Erlangen, Germany). In order to reach consensus, image interpretation was performed by two radiologists (J.V. with 5 years and J.F.S. with 10 years of experience in chest radiology), firstly the MRI of all cases and, secondly, the CT. For the MRI images, an individual window and center was used optimizing the contrast for internal and external lesion evaluation. The CT images were displayed in standard lung (W 1500 HU, C – 500 HU) and mediastinal window (W 350 HU, C 50 HU).

For the evaluation of the pulmonary lesions the shapes, the external and internal structures as well as the periphery of the nodules were assessed [15-20]. The shape was classified as round-ovoid or not, i.e. lobular, notched or irregular. The margin was categorized as either smooth or not, i.e. indistinct, irregular or spiculated. The presence of spicules was evaluated. The internal structures were assessed by analysis of homogeneity (homogeneous or inhomogeneous) and the presence of cavitations. The periphery of the nodules was characterised by the presence of ground-glass opacity, satellite nodules, bronchus sign and vessel sign. Satellite nodules were defined as one or more distinctly separate nodular area observed within a distance of 5 mm from the lesion. The bronchus sign was defined as a visible bronchus leading to the nodule and the vessel sign as a pulmonary vein leading to the nodule. The visceral pleura was analysed for the presence of thickening or retraction, as well as for the presence of spicules connecting lesion and pleura.

Analysis for Differentiation between Malignant and Benign SPN

To investigate the diagnostic accuracy for both modalities in differentiation between malignant and benign SPN and the diagnostic confidence, three radiologists subsequently evaluated the images. The degree of experience in diagnostic radiology varied (12 years, 9 years and 6 years). They had no contact to the study and were blinded to all results. Firstly, the MRI examination was analyzed in two sessions with a time interval of 4 weeks in order to reduce the recall bias. Secondly, after 4 weeks, the CT images were scrutinized likewise in two sessions with a similar time interval. For each case, the observers made a diagnosis in every session using a five point score. The definition simulating a clinical setting was as follows: one point was defined as benign, follow up in one year or later. Two points was defined as probably benign, follow up in less than one year. Three points was defined as indeterminate, but possibly malignant, follow up in shorter interval or invasive diagnostic. Four points was defined as probably malignant and five points as malignant. In both latter circumstances, a histological confirmation would be necessary. The definition was printed out on the evaluation form for each case. Diagnostic level of confidence was defined as low for three points, medium for two or four points, and high for one or five points. To calculate the diagnostic accuracy, the five point analysis was summarized, where one and two points represented benign SPN and three to five points represented malignant SPN.

Statistical Analysis

The statistical evaluation was carried out with version 4.0.4 of the program JMP (SAS Institute Inc., USA, 2001). The Generalized Fisher's exact test was used for analysis in the differences of morphologic signs between benign and malignant SPN with descriptive P-value less than 0.05. As some morphological signs are strongly associated with each other, we also used multivariate U-scores in order to compute ROC curves. Signs present and absent in more than 3/46

patients were incorporated here. Sensitivity, specificity and accuracy were calculated from the results of the reading sessions of the three radiologists. To compare the diagnostic accuracy of both modalities, a sign-test was used. The effects of modality (CT vs. MRI), session number (one or two) and observers (1,2 and 3) on sensitivity, specificity and diagnostic confidence were estimated in multiple logistic regressions.

RESULTS

Frequency of malignant nodules in the cohort was 52% (24/46) of nodules (Table 1). Table 2 summarizes the results of the morphologic evaluation for both methods. For MRI, a significant differentiation between malignant and benign lesions was possible with the following signs: round-ovoid shapes, smooth margins, inhomogeneities and vessel signs (all P values < 0.05). For CT, the best characteristics were round-ovoid shape, smooth margin, and presence of spicules, vessel sign and spicules with extension to pleura (all P values < 0.05). Figures 1 to 4 demonstrate exemplary the specific findings of MRI compared to CT. Areas

Table 1. Diagnosis and Number of SPNs.

Diagnosis	No. of Nodules	
All Nodules	46	(100%)
Malignant	24	(52%)
Adenocarcinoma	8	(17%)
Squamous cell carcinoma	7	(15%)
Small cell carcinoma	3	(7%)
Carcinoid	1	(2%)
Metastases	5	(11%)
Benign	22	(48%)
Hamartoma	12	(26%)
Observations	3	(7%)
Inflammatory lesion	5	(11%)
Inactive tuberculoma, Intrapulmonary lymph node	2	(4%)

Table 3. Effect test P values of 3 logistic regressions from sensitivity, specificity and subjective diagnostic confidence on, reading session, reader and modality.

Parameter	Sensitivity	Specificity	Confidence
Session	0.26	0.67	0.53
Reader	0.74	<0.01	0.01
Modality	0.10	0.66	<0.01

Table 4. Results of readers sensitivity, specificity and accuracy for MRI and helical CT.

	Sensitivity	Specificity	Accuracy
MRI Reader 1	90 (22/24)	37 (8/22)	64 (29/46)
MRI Reader 2	88 (21./24)	30 (7/22)	61 (28/46)
MRI Reader 3	88 (21./24)	59 (13/22)	74 (34/46)
MRI Mean	89 (21/24)	42 (9/22)	66 (30./46)
CT Reader 1	92 (22./24)	34 (7/22)	64 (29/46)
CT Reader 2	92 (22./24)	30 (7/22)	63 (29/46)
CT Reader 3	96 (23./24)	59 (13/22)	78 (36/46)
CT Mean	95 (23/24)	41 (9/22)	68 (31/46)

Table 2. Results of morphological evaluation of 24 malignant and 22 benign SPN for helical CT and MRI.

	Helical CT			MRI		
	Benign	Malign.	P value	Benign	Malign.	P value
External Characteristic						
Shape						
Round/ovoid	12 (54)	5 (21)	0.03	11 (50)	2 (8)	0.017
Margin						
Smooth	18 (82)	3 (12.5)	<0.0001	16 (73)	6 (25)	0.0027
Spicules						
Present	4 (18)	19 (79)	< 0.0001	4 (18)	11 (46)	0.063
Internal Characteristic						
Inhomogeneity	5 (23)	11 (46)	0.13	10 (45)	20 (83)	0.012
Cavitation	1 (5)	3 (13)	0.61	1 (5)	1 (4)	1
Peripheral Characteristic						
Ground-glass-opacity	4 (18)	11 (46)	0.063	0 (0)	2 (8)	0.49
Bronchus sign	5 (23)	12 (50)	0.072	1 (5)	2 (8)	1
Vessel sign	2 (9)	14 (58)	0.0006	0 (0)	6 (25)	0.022
Satellite nodules	1 (5)	2 (8)	1	1 (5)	1 (5)	1
Spicules to the pleura	3 (14)	15 (63)	0.0009	2 (9)	6 (25)	0.25
Pleura thickening	3 (14)	9 (38)	0.096	1 (5)	6 (25)	0.098

Note. Numbers in parentheses are percentages

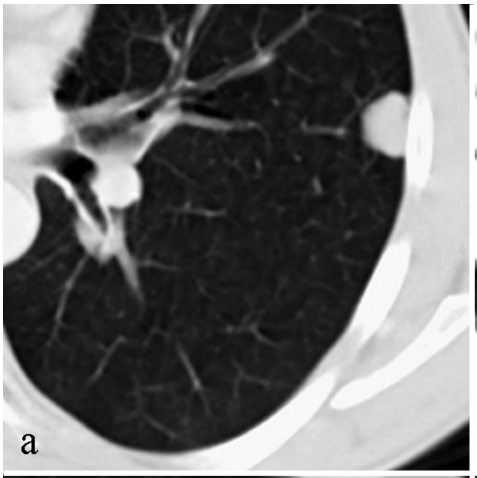

Fig. 1. Images of a 50 year old man showing an example of a round-ovoid nodule with smooth margins of the left upper lobe. Note the diameters are identical (15 mm). Histological, a hamartoma was found. (a) CT, (b) MRI.

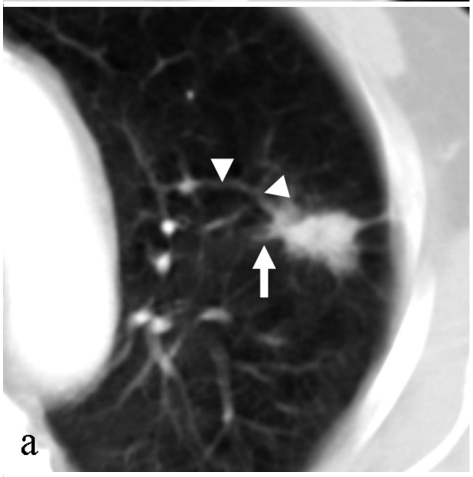

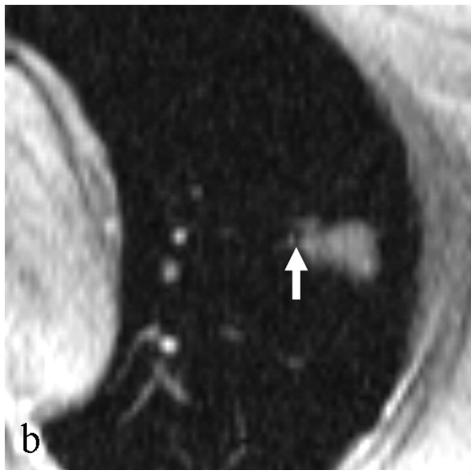

Fig. 2. Images of a 59 year old man revealing differences between MRI and CT for both diameter and morphology. In CT, irregularly shaped lesion of left upper lobe (mean diameter 19.5 mm) with spicules extending to the pleura and pleura retraction is visible. Note positive finding of vessel (arrowhead) and bronchus sign (arrow). In MRI, the nodules appear smaller (mean diameter 17.5 mm) and show no spicules, but irregular margins. Note the bronchus sign but not the vessel sign is positive. Histological, an adenocarcinoma was found. (a) CT, (b) MRI.

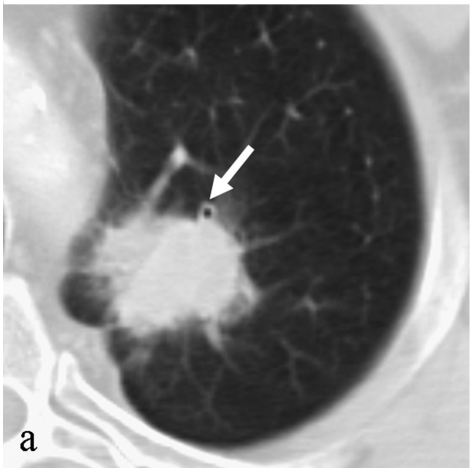

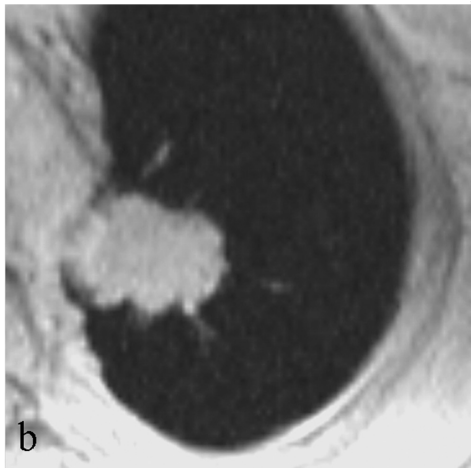

Fig. 3. Images of a 47 year old man revealing a similarity of appearance in both methods showing spicules with extension to the pleura and pleura thickening. Note the adjacent bronchus (arrow) is not seen in MRI. The 35 mm mass was a squamous cell carcinoma. (a) CT, (b) MRI.

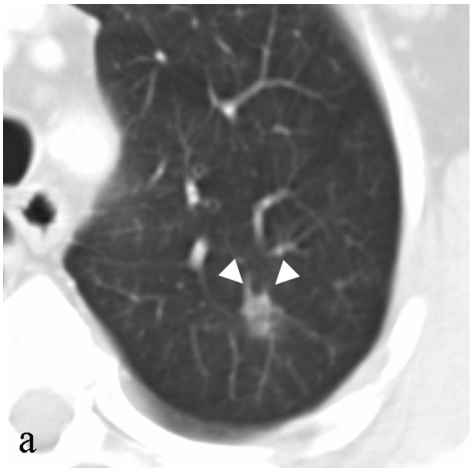

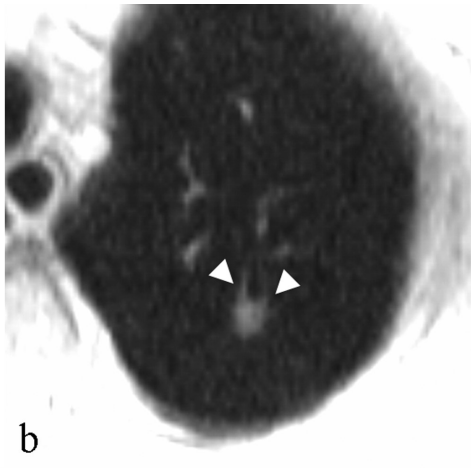

Fig. 4. Images of a 62 year old man revealing the vessel sign in both modalities. Two veins draining the nodule in the left upper lobe (8 mm in size) are noted by arrowheads. Histological, an adenocarcinoma was found. (a) CT, (b) MRI.

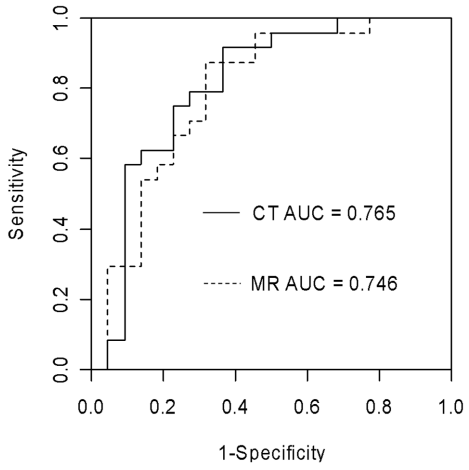

Fig. 5. ROC Analyses of diagnostic accuracy of MRI and CT using multivariate U-scores for signs present and absent in more than 3/46 patients.

under ROC curves computed from multivariate U-scores were 0.746 for MRI and 0.765 for CT (Fig. 5).

The session number shows no significant effect on observer's diagnostic accuracy (Table 3). Therefore, the results are listed as mean results from both sessions in Table 4. The sensitivity for MRI ranged from 88% to 90% and for CT from 92% to 96%. The specificity for both ranged from 30% to 59%. The mean accuracy for MRI was 66% and for CT 68%.

The results of sensitivity were found independently from modalities and observer. For specificity, a significant effect of observer experience was present ($P = 0.001$). The odds ratio for observers 1, 2 and 3 against the mean were 0.07, 0.23 and 65.68. The latter was most experienced in diagnostic radiology.

No significant difference between CT and MRI was found. For all nodules, the results differed in 60 of 276 (22%) pairs between the modalities ($P = 0.44$). From these 60 discordant pairs, 27 (45%) were true for MRI and 37 (55%) true for CT. For malignant nodules 11% (17/144) and for benign nodules 33% (43/132) of pairs were discordant ($P = 0.09$ and $P = 0.88$).

The diagnostic confidence was different for the modalities ($P < .01$) (Table 3). The vote of all observers for an indeterminate nodule (score 3) was higher in MRI with 33% than in CT with 27%. Furthermore, the vote for a probable benign or malignant lesion was more present in MRI (60%) compared with CT (48%), whereas nomination of the highest confidence (score 1 or 5) was more frequent for CT (25% vs. 7%). Additionally, the influence of observer experience was found to be significant ($P = 0.01$).

Discussion

The study aimed to evaluate the possibilities MRI in morphologically characterization of SPN using classical sign. The results demonstrated that MRI allows a differentiation between benign and malignant lesions with a high sensitivity and a moderate specificity. No relevant difference in comparison to conventional helical CT was observed, when the accuracies of the independent radiologist reading sessions were compared.

With the use of CT, we observed a useful discrimination between malignant and benign nodules by a round or ovoid shape, as well as a smooth margin which concur with previous results [16-18, 20]. These findings were not seen in a former HRCT study [19]. One possible cause may be the larger slice thickness and the higher number of hamartomas in the benign group in our study. Results agree in that the presence of spicules and their extension to the pleura are criteria for malignancy. Furthermore, we could confirm the frequency of the vessel sign for malignant nodules. We found the vessel sign in 58% (12 primary lung cancer and 2 metastases), being similar to the corresponding value of the investigations by a former HRCT study (70%) [19]. Mori et al. found the vessel sign in 93% of primary lung cancers [15]. Not statistically significant but dominant in malignancy as in previous studies were inhomogeneous nodules, cavitations, satellite nodules, ground glass opacity adjacent to the nodule and pleural thickening or retraction [19, 21, 22].

Some methodical limitations of the used CT techniques have to be considered, as in our study no HRCT was evaluated and no state of the art multi-row CT was available. On the other hand, the recent literature has not shown a relevant advantage of these techniques over standard helical CT for differentiation between benign and malignant SPN, when only morphologic criteria in solid SPN were evaluated [23, 24]. Furthermore, the single slice technique is, until now, still widely used and is often the standard procedure in the diagnostic work up of pulmonary nodules. The frequency of malignancy of 52% in our study was lower than or similar to that of former investigations [15, 19, 21, 22, 25] enhancing the results regarding specificity.

The choice of the field strength plays an important role in lung imaging. As magnetic susceptibility is proportional to B_0, a low field scanner would be especially useful for lung imaging [26]. Unfortunately, signal intensity is also proportional to field strength. For this reason, the scanner used in this study with intermediate field strength of 1.0 Tesla may be a good compromise. Nevertheless, the effect of magnetic susceptibly seems to be directly responsible for differences between CT and MRI leading to signal loss on the edges of the nodule. Therefore, particularly spicules and pleural reaction were not delineated in the same manner as in CT. Additionally, a low proton density of spicules due to desmoplastic response of the lung tissue has to be taken into account, which can also mimic ground glass attenuation [27]. In spite of these difficulties in MRI, a differentiation between smooth and not smooth margins (i.e. indistinct or irregular) was possible. Using those signs, which allow a significant differentiation ($p < 0.05$) between malignant and benign nodules in CT or MRI, comparable AUCs were achieved.

No significant effect of image modality on observer diagnostic accuracy was observed. Between MRI and CT, the percentage of discordance was 22% (60/276) of all pairs, where 45% (27/60) MRI and 55% CT (33/60) found the truth. Furthermore, the effect of observer experience was not different between MRI

and CT, showing no significant influence on results of sensitivity, but, on specificity for both modalities. The mean sensitivities of both modalities were comparable to the investigation of Seemann et al., who found a sensitivity of 91% [19]. The range of observer sensitivities was low (2 % for CT and 4% for MRI), whereas a high range was found for specificity (29 % for both methods). Only the experienced observer reached a specificity of 59 %, which is similar to previously reported results [19]. In a clinical setting, which we have attempted to simulate by the definition of the score, a high sensitivity with low inter observer range and low specificity with a high range are no surprise, when only morphologic signs are used to differentiate malignant from benign SPN. Thus, a high percentage of surgically removed lesions are benign [28].

One reason for these promising results of MRI in this study is the optimized signal gain using a proton density weighted GE with a short echo time and a low flip angle. However, due to the lower spatial resolution of MRI compared to CT with pixel size of 1.3 mm, the visualization of nodule characteristics was limited. True (not interpolated) higher spatial resolution is difficult to achieve due to the disadvantages such as an increase of acquisition time leading to motion artifacts or decreasing the SNR. Another possible reason explaining the high accuracy of MRI in our results is the use of ECG-triggering. We did not observe disturbing pulsation artifacts, which are one of the evident difficulties in lung imaging, particularly when the lesion is located centrally. Thus, due to the relatively sharp delineation of nodules and pulmonary veins (unlike trigger delay), the vessel sign was seen in 6 of 14 positive nodules in CT. The main disadvantages of our approach are the relatively long acquisition time and the need for cooperative patients.

Although new possibilities such as parallel imaging (PAT) (which was not available at the beginning of this study) shortens the acquisition time, it cannot solve the problems completely due to a decrease in signal intensity particularly in the lung with its low proton density. Another more new approach using a 3D GE, the so called VIB (volume interpolated breath hold) sequences, is promising in pulmonary imaging [29]. Although, a higher spatial resolution could be achieved using this sequence type by interpolation, pulsation artifacts cannot completely be reduced [29]. Other different MRI techniques have been used for visualization of pulmonary nodules. However, fast spin echo sequences (SE) or half-Fourier single-shot fast SE (HASTE) are relatively insensitive to magnetic susceptibility due to repetitive rephasing, but the first approach needs respiratory and cardiac triggering and the latter shows image blurring due to a reduction of resolution in phase encoding direction by the filtering SI from tissue with short T2 relaxation time.

Our study has, however, some limitations: (a) although the MRI data acquisition was prospective, the morphologic analyses were performed retrospectively (b) CT data were heterogeneous and only conventional helical scanners were used, (c) a selection bias must be considered due to the fact that departments of surgery referred numerous hamartomas, (d) the evidence of the results is limited by the relative small sample.

The present study focused on the morphological characteristics of SPN using an ECG gated gradient echo sequence. Using these characteristics for the differentiation between malignant and benign SPN, the diagnostic performance of MRI was found comparable to conventional helical CT. Further investigations are necessary to demonstrate the clinical use of our results in combination with functional parameters (i.e. contrast enhancement), establishing MRI as a comprehensive diagnostic modality for SPN.

REFERENCES

1. Martirosian P, Boss A, Fenchel M, Deimling M, Schafer J, Claussen CD, Schick F (2006) Quantitative lung perfusion mapping at 0.2 T using fair true-FISP MRI. Magn Reson Med 55:1065-1074
2. Bergin CJ, Glover GM, Pauly J (1993) Magnetic resonance imaging of lung parenchyma. J Thorac Imaging 8: 12-17
3. Hatabu H, Chen Q, Stock K, Gefter W, Itoh H (1999) Fast magnetic resonance imaging of the lung. Eur J Radiol 29:114-132
4. Gaa J, Rummeny EJ, Seemann MD (2004) Whole-body imaging with PET/MRI. Eur J Med Res 9:309-312
5. Schlemmer H, Schafer J, Pfannenberg C, Radny P, Korchidi S, Muller-Horvat C, Nagele T, Tomaschko K, Fenchel M, Claussen C (2005) Fast whole-body assessment of metastatic disease using a novel magnetic resonance imaging system: Initial experiences. Invest Radiol 40:64-71
6. Seemann MD, Meisetschlaeger G, Gaa J, Rummeny EJ (2006) Assessment of the extent of metastases of gastrointestinal carcinoid tumors using whole-body PET, CT, MRI, PET/CT and PET/MRI. Eur J Med Res 11:58-65
7. Kersjes W, Mayer E, Buchenroth M, Schunk K, Fouda N, Cagil H (1997) Diagnosis of pulmonary metastases with turbo-SE MR imaging. Eur Radiol 7:1190-1194
8. Lutterbey G, Leutner C, Gieseke J, Rodenburg J, Elevelt A, Sommer T, Schild H (1998) Detection of focal lung lesions with magnetic resonance tomography using T2-weighted ultrashort turbo-spin-echo-sequence in comparison with spiral computerized tomography. Fortschr Rontgenstr 169:365-369
9. Schafer JF, Vollmar J, Schick F, Seemann MD, Kamm P, Erdtmann B, Claussen CD (2005). Detection of pulmonary nodules with breath-hold magnetic resonance imaging in comparison with computed tomography. Fortschr Rontgenstr 177:41-49
10. Vogt F, Herborn C, Hunold P, Lauenstein T, Schroder T, Debatin J, Barkhausen J (2004) Haste MRI versus chest radiography in the detection of pulmonary nodules: Comparison with MDCT. AJR Am J Roentgenol 183:71-78
11. Ohno Y, Hatabu H, Takenaka D, Adachi S, Kono M, Sugimura K.(2002) Solitary pulmonary nodules: Potential role of dynamic MR imaging in management initial experience. Radiology 224:503-511
12. Schaefer JF, Vollmar J, Schick F, Vonthein R, Seemann MD, Aebert H, Dierkesmann R, Friedel G, Claussen CD (2004) Solitary pulmonary nodules: Dynamic contrast-enhanced MR imaging--perfusion differences in malignant and benign lesions. Radiology 232:544-553
13. Kim JH, Kim HJ, Lee KH, Kim KH, Lee HL (2004) Solitary pulmonary nodules: A comparative study evaluated with contrast-enhanced dynamic MR imaging and CT. J Comput Assist Tomogr 28:766-775
14. Tozaki M, Ichiba N, Fukuda K (2005) Dynamic magnetic resonance imaging of solitary pulmonary nodules: Utility of kinetic patterns in differential diagnosis. J Comput Assist Tomogr 29:13-19

15. Mori K, Saitou Y, Tominaga K, Yokoi K, Miyazawa N, Okuyama A, Sasagawa M (1990) Small nodular lesions in the lung periphery: New approach to diagnosis with CT. Radiology 177:843-849
16. Zwirewich CV, Vedal S, Miller RR, Muller NL (1991) Solitary pulmonary nodule: High-resolution CT and radiologic-pathologic correlation. Radiology 179:469-476
17. Siegelman SS, Khouri NF, Leo FP, Fishman EK, Braverman RM, Zerhouni EA (1986) Solitary pulmonary nodules: CT assessment. Radiology 160:307-312
18. Zerhouni EA, Stitik FP, Siegelman SS, Naidich DP, Sagel SS, Proto AV, Muhm JR, Walsh JW, Martinez CR, Heelan RT, et al (1986) CT of the pulmonary nodule: A cooperative study. Radiology 160:319-327
19. Seemann MD, Staebler A, Beinert T, Dienemann H, Obst B, Matzko M, Pistitsch C, Reiser MF (1999) Usefulness of morphological characteristics for the differentiation of benign from malignant solitary pulmonary lesions using HRCT. Eur Radiol 9:409-417
20. Erasmus JJ, Connolly JE, McAdams HP, Roggli VL (2000) Solitary pulmonary nodules: Part I. Morphologic evaluation for differentiation of benign and malignant lesions. Radiographics 20:43-58
21. Siegelman SS, Zerhouni EA, Leo FP, Khouri NF, Stitik FP (1980) CT of the solitary pulmonary nodule. AJR Am J Roentgenol 135:1-13
22. Zwirewich C, Vedal S, Miller R, Muller N (1991) Solitary pulmonary nodule: High-resolution CT and radiologic-pathologic correlation. Radiology 179:469-476
23. Seemann MD, Seemann O, Luboldt W, Bonel H, Sittek H, Dienemann H, Staebler A (2000) Differentiation of malignant from benign solitary pulmonary lesions using chest radiography, spiral CT and HRCT. Lung Cancer 29:105-124
24. Tsubamoto M, Johkoh T, Kozuka T, Honda O, Koyama M, Murai S, Inoue A, Sumikawa H, Tomiyama N, Hamada S, Yamamoto S, Nakamura H, Kudo M (2003) Coronal multiplanar reconstruction view from whole lung thin-section ct by multidetector-row CT: Determination of malignant or benign lesions and differential diagnosis in 68 cases of solitary pulmonary nodule. Radiat Med 21:267-271
25. Takanashi N, Nobe Y, Asoh H, Yano T, Ichinose Y (1995) The diagnostic accuracy of a solitary pulmonary nodule, using thin-section high resolution CT: A solitary pulmonary nodule by HRCT. Lung Cancer 13:105-112
26. Kveder M, Zupancic I, Lahajnar G, Blinc R, Suput D, Ailion DC, Ganesan K, Goodrich C (1988) Water proton NMR relaxation mechanisms in lung tissue. Magn Reson Med 7:432-441
27 Sone S, Sakai F, Takashima S, Honda T, Yamanda T, Kubo K, Fukasaku K, Maruyama Y, Li F, Hasegawa M, Ito A, Yang Z (1997) Factors affecting the radiologic appearance of peripheral bronchogenic carcinomas. J Thorac Imaging 12:159-172
28. Decamp MM Jr (2002) The solitary pulmonary nodule: Aggressive excisional strategy. Semin Thorac Cardiovasc Surg 14:292-296
29. Both M, Schultze J, Reuter M, Bewig B, Hubner R, Bobis I, Noth R, Heller M, Biederer J (2005) Fast t1- and t2-weighted pulmonary MR-imaging in patients with bronchial carcinoma. Eur J Radiol 53:478-488

Received: August 28,2006 / Accepted: September 11, 2006

Address for correspondence:
Juergen F. Schaefer
Department of Diagnostic Radiology
University of Tuebingen
Hoppe- Seyler-Str. 3
72076 Tuebingen, Germany
Phone: +49/7071/2982087
Fax: +49/7071/295845
E-Mail: juergen.schaefer@med.uni-tuebingen.de